PROCEEDINGS OF SCIENCE

Towards multi-messenger observations of core-collapse supernovae harbouring choked jets

Angela Zegarelli,[a,*] **Dafne Guetta,**[b] **Silvia Celli,**[c,d] **Silvia Gagliardini,**[b,c,d] **Irene Di Palma**[c,d] **and Imre Bartos**[e]

[a] *Ruhr University Bochum, Faculty of Physics and Astronomy, Astronomical Institute (AIRUB), Universitätsstraße 150, 44801, Bochum, Germany*

[b] *Department of Physics, Ariel University, Ariel, Israel*

[c] *INFN, Istituto Nazionale di Fisica Nucleare, Sezione di Roma, P. le Aldo Moro 2, I-00185, Roma, Italy*

[d] *Dipartimento di Fisica, Università La Sapienza, P. le Aldo Moro 2, I-00185, Roma, Italy*

[e] *Department of Physics, University of Florida, Gainesville, FL 32611-8440, USA*

E-mail: angela.zegarelli@astro.ruhr-uni-bochum.de

Over the last decade, the scenario of choked jets embedded in core-collapse supernovae (CCSNe) has garnered significant attention. The extended stellar envelopes of red supergiant (RSG) and blue supergiant (BSG) stars, both progenitors of Type II supernovae, pose a challenge to the launch of a powerful jet capable of piercing through them. As the jet propagates, it dissipates energy in a double-shock structure that forms at its head. The hot material at the jet's head spills sideways, creating a cocoon that engulfs and collimates the jet. If the jet traverses a significant fraction of the stellar envelope before choking, the cocoon can become energetic enough to break out of the star, producing ultraviolet (UV) and optical emissions that persist for several days. Identifying both these electromagnetic signals is crucial for characterizing RSGs and BSGs, given the low probability of gamma rays escaping.

Here, we discuss the prospects of measuring UV emission in light of the upcoming launch of the ULTRASAT satellite, which will operate in the UV band and complement the capabilities of the currently active optical telescope ZTF. Furthermore, choked jets are of great interest in the growing field of multi-messenger astronomy, as they are considered potential contributors to the astrophysical diffuse neutrino flux, which remains unassociated with any known source. In this context, I explore the potential of multi-messenger observations to optimize joint detections across UV, optical, and neutrino telescopes, enhancing synergy between different observational facilities.

39th International Cosmic Ray Conference (ICRC2025)
15–24 July 2025
Geneva, Switzerland

*Speaker

PoS(ICRC2025)1225

This contribution is based on the study published in [1, 2], where the full analysis and methodological details are provided.

1. Introduction

At the end of their lives, massive stars (with initial masses $\gtrsim$8 solar masses) typically undergo core collapse, forming a compact object such as a neutron star or a black hole. Accretion of stellar material onto this remnant can power a highly energetic, relativistic outflow. When the progenitor has lost its outer hydrogen and helium layers through strong stellar winds, the collapse leads to a Type Ib/c supernova (SN), often associated with long gamma-ray bursts (GRBs), the most luminous explosions in the Universe. However, if the star retains its outer layers, the collapse results in a Type II SN. In such cases, relativistic jets may fail to escape the stellar envelope and remain *choked*.

As the jet propagates through the star, material accumulates at its head and flows sideways, inflating a hot, pressurized *cocoon* that collimates the jet and can, in some cases, break out of the star even if the jet itself does not. Although choked jets are highly optically thick to gamma (γ) rays, they can still produce observable emission via the surrounding cocoon. This may result in a distinct electromagnetic signature: a bright X-ray or UV flash lasting from a few seconds to tens of minutes, followed by longer-lived UV/optical emission on day-long timescales, powered by the expanding cocoon. In any case, the emergence of an electromagnetic signal requires that the shock successfully reaches the stellar surface [3].

In addition to their electromagnetic counterparts, choked jets can produce high-energy neutrinos through hadronic interactions occurring within the jet prior to breakout. These neutrinos, typically in the TeV–PeV range, escape the progenitor promptly and are not accompanied by γ-ray emission, which is suppressed by intense photon fields inside the star [4]. As a result, choked jets are compelling candidates for the so-called hidden sources of cosmic neutrinos, i.e., sources that evade constraints from the diffuse γ-ray background observed by the *Fermi* satellite [5, 6].

In this work, we focus on core-collapse SNe (CCSNe) from blue supergiant (BSG) and red supergiant (RSG) progenitors, which are characterized by extended, H-rich envelopes and negligible circumstellar material (CSM), under the hypothesis that such envelopes can host choked relativistic jets [e.g. 7, 8]. We assess whether the associated shock breakout (SBO) emission, produced when the cocoon-driven shock reaches the stellar surface, can be detected through a multi-messenger approach that combines high-energy neutrino alerts with UV/optical follow-up. Such strategies may offer a unique opportunity to uncover the origin of part of the cosmic neutrino flux, discovered in 2013 [9] and still not fully associated with known astrophysical sources, and to probe the physics of stellar explosions.

In Sec. 2, we outline the method developed to assess the detectability of UV and optical signals from choked jets, the corresponding results, and the implementation of a multi-messenger framework, including also high-energy neutrinos, aimed at maximizing observational prospects. In Sec.3, we discuss the implications of our results.

2. Multi-messenger detectability of shock-cooling emission from choked jets in CCSNe

Testing the hypothesis that choked jets are potential sources of high-energy cosmic neutrinos through a multi-messenger approach is particularly challenging due to the absence of an accompa-

nying γ-ray counterpart, making the identification of alternative electromagnetic signatures crucial. In this context, we explore the detectability of associated UV and optical emissions, which provide critical insights into the early evolution of choked jets by tracing the energy released as shock waves interact with the stellar envelope. These emissions offer valuable information on the dynamics and physical conditions of such explosive events.

This investigation is especially timely with the planned 2028 launch of the Ultraviolet Transient Astronomy Satellite (ULTRASAT) [10], which will fill a major observational gap. Operating in the near-UV with an unprecedented ~200 deg^2 field of view, ULTRASAT will enable wide-field UV monitoring of CCSNe and potential choked-jet progenitors, unlocking new opportunities for detailed study. While it is uncertain whether the Zwicky Transient Facility (ZTF) will remain operational by ULTRASAT's launch, we assess the scientific prospects of combining ULTRASAT data with those from high-performance optical facilities such as ZTF or similar next-generation instruments, alongside contemporaneous neutrino observations. This multi-messenger synergy is crucial to fully exploit ULTRASAT's discovery potential and to advance our understanding of the electromagnetic and neutrino signatures of choked-jet-driven explosions. We advocate for a coordinated follow-up strategy integrating UV, optical, and neutrino data, which will be essential to identify candidate sources and develop effective approaches for detecting and interpreting these complex phenomena.

In Sec. 2.1, we summarize the model adopted to describe the UV and optical cooling emission following the SBO. In Sec. 2.2, we evaluate the detection prospects of this emission with ULTRASAT and ZTF, including estimates of the expected event rates for both instruments. In Sec. 2.3, we discuss how high-energy neutrino observations can be integrated into a multi-messenger strategy combining UV, optical, and neutrino data, and involving coordinated efforts across different observatories.

2.1 UV and optical emission from shock breakout flares in hydrogen-dominated stellar envelopes

We consider the early UV and optical emission produced as the stellar envelope expands and cools following the SBO, focusing on hydrogen-rich envelopes typical of RSGs and BSGs [11, 12]. As the photosphere recedes through the outer layers of the expanding envelope, the adiabatically cooled radiation stored within escapes, producing UV and optical emission on timescales of days.

The specific intensity observed at Earth, f_λ, is modeled as blackbody radiation modified by extinction due to dust and gas along the line of sight:

$$f_\lambda(\lambda, t) = \left(\frac{r_{\rm ph}}{D_L(z)}\right)^2 \sigma T_{\rm ph}^4 \frac{T_{\rm col}}{hc} g_{BB}(x) e^{-\tau_\lambda}, \tag{1}$$

where $D_L(z)$ is the luminosity distance at redshift z, $T_{\rm col}$ is the color temperature,[1] and τ_λ is the wavelength-dependent optical depth. Here, σ is the Stefan–Boltzmann constant, h is the Planck constant, and c is the speed of light. The function $g_{BB}(x)$ represents the normalized blackbody spectrum:

$$g_{BB}(x) = \frac{15}{\pi^4} \frac{x^5}{e^x - 1}, \tag{2}$$

[1] The color temperature corresponds to the temperature of a blackbody emitting radiation with the same spectral shape as the source.

with $x = hc/(\lambda T_{\rm col})$. The time evolution of the photospheric radius $r_{\rm ph}$ and effective temperature $T_{\rm ph}$ depend on the envelope's radial extension R_*,the kinetic energy released E and mass ejected $M_{\rm ej}$ during the supernova explosion, the time elapsed since the SBO t, and a parameter f_ρ, which is a numerical factor of order unity that depends on the inner envelope structure and density profile. These parameters are computed following the full expressions provided in our paper [1].

2.2 Detection prospects of UV and optical emission with ULTRASAT and ZTF

To evaluate how feasible it will be to detect early UV and optical signatures of SBO from choked-jet SNe, we assess the detectability of the modelled emission with upcoming and existing instruments. In particular, we focus on ULTRASAT, whose wide field of view and near-UV sensitivity make it especially well suited for capturing the prompt emission associated with SBO events. This is particularly relevant for identifying choked jets, which lack a gamma-ray counterpart and thus rely on alternative electromagnetic tracers. We aim to determine whether the UV and optical emission produced as the stellar envelope cools, following the SBO and powered by a choked jet, can be observed with ULTRASAT and optical surveys such as ZTF.

We assess detectability by comparing the predicted specific intensity f_λ from our model (see Eq. 1) with the limiting flux sensitivities of ULTRASAT and optical surveys such as ZTF, expressed in terms of AB magnitudes. The AB magnitude $m_{\rm AB}$ is related to the flux density f_ν as:

$$m_{\rm AB} = -2.5 \log_{10}\left(\frac{f_\nu}{[\rm Jy]}\right) + 8.90, \tag{3}$$

and f_ν is converted to f_λ via:

$$\frac{f_\nu}{[\rm Jy]} = 3.34 \times 10^4 \left(\frac{\lambda}{\text{Å}}\right)^2 \frac{f_\lambda}{[\rm erg\ cm^{-2}\ s^{-1}\ Å^{-1}]}. \tag{4}$$

We adopt a pivot wavelength of 260 nm for ULTRASAT and filter-specific values from the Spanish Virtual Observatory (SVO) Filter Profile Service[2] for ZTF. Both yield a detection threshold of approximately $f_\lambda^{\rm lim} \simeq 2 \times 10^{-9}$erg cm^{-2}s^{-1}Å^{-1}.

To model the emission in Eq. 1, we adopt fiducial parameters for RSGs and BSGs:

- For RSGs, values are based on SN II light curves with UV and optical detections fitted using the same shock-cooling model [13]: $R_* = 722\,R_\odot$, $E = 10^{51}$ erg, $M_{\rm ej} = 2.8\,M_\odot$, and $f_\rho = 1.455$.
- For BSGs, due to the lack of constraints, we adopt representative theoretical parameters [14]: $R_* = 50\,R_\odot$, $M_{\rm ej} = 10\,M_\odot$, $E = 10^{51}$ erg, and $f_\rho = 0.0465$.

We also account for extinction using the wavelength-dependent curve from [15], assuming a Milky Way-like interstellar medium with $R_V = 3.1$. Based on 1773 SN II hosts from the ZTF Bright Transient Survey, we adopt a benchmark value of $E_{B-V} = 0.04^{+0.21}_{-0.03}$.

As a result of this procedure, Figure 1 shows the expected extinction-corrected f_λ at different times after the SBO occurrence as a result of the outer stellar envelope cooling of RSG and BSG stars. The duration of the SBO can be roughly estimated as the progenitor light-crossing time ($\Delta t_{\rm SBO} \simeq R_*/c$). For the set of fiducial parameters we adopted, $\Delta t_{\rm SBO} \sim 30(2)$ minutes for

[2]The SVO collects, standardizes, and distributes transmission profiles of photometric filters used by a wide range of telescopes and astronomical surveys: http://svo2.cab.inta-csic.es/svo/theory/fps/.

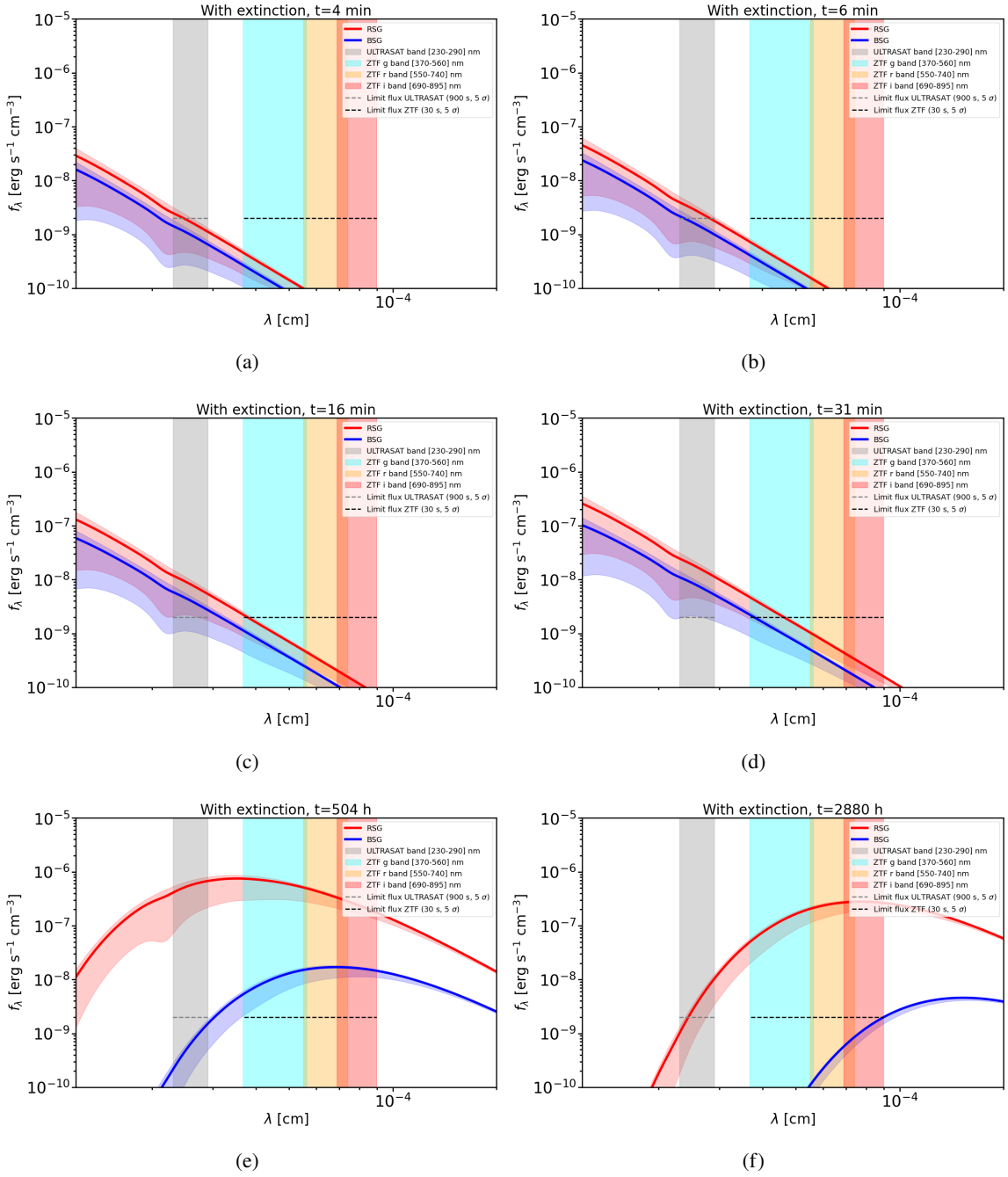

Figure 1: Extinction-corrected specific intensities, f_λ, observable at Earth from a RSG (in red) and BSG (in blue) located at $z = 0.01$, as expected from the model in Eq. (3). The fiducial parameters used in the computation for RSGs are $R_* = 722\ R_\odot$, $E = 10^{51}$ erg, $M_{\rm ej} = 2.8\ M_\odot$, and $f_\rho = 1.455$, and for BSGs $R_* = 50\ R_\odot$, $M_{\rm ej} = 10\ M_\odot$, $f_\rho = 0.0465$, and $E = 10^{51}$ erg. The solid lines show the expected emission with a median Galactic extinction $E_{B-V} = 0.04$, and the corresponding shaded region the minimum and maximum extinction values, i.e. $E_{B-V} = 0.01$ and $E_{B-V} = 0.25$, respectively. The vertical shaded bands represent the wavelength range covered by each instrument: ULTRASAT (in grey) and ZTF with the *g* filter (in cyan), *r* filter (in yellow), and *i* filter (in red). The horizontal dashed grey and black lines define the $f_\lambda^{\rm lim}$ of the two instruments, obtained following Eq. (7). Panels (a) to (f) show the different evolution times, from ~ 5 minutes to ~ 4 months after the SBO event, highlighting for each stellar progenitor the time range when the emission was visible to ULTRASAT and ZTF..

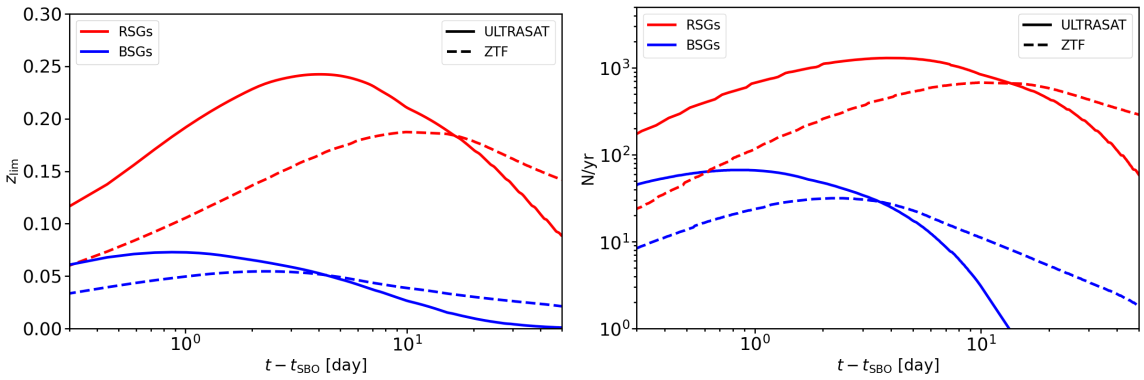

(a) (b)

Figure 2: Capability of detecting UV and optical emission from RSGs and BSGs with ULTRASAT and ZTF. (a) Maximum redshift at which RSGs and BSGs would have UV and optical emissions detectable by ULTRASAT and ZTF as a function of the emission time, t. (b) Rate of SNe II per year from RSGs and BSGs detectable with ULTRASAT and ZTF as a function of the emission time, t. In both panels, the following fiducial parameters are adopted: for RSGs $R_* = 722\ R_\odot$, $E = 10^{51}$ erg, $M_{\rm ej} = 2.8\ M_\odot$, and $f_\rho = 1.455$; for BSGs $R_* = 50\ R_\odot$, $M_{\rm ej} = 10\ M_\odot$, $f_\rho = 0.0465$, and $E = 10^{51}$ erg. The emission time corresponds to the time elapsed since the SBO. Results for RSGs and BSGs are shown in red and blue, respectively. The solid and dashed lines show ULTRASAT and ZTF results, respectively.

RGSs(BSGs). Here, a median redshift of $z = 0.01$ (luminosity distance of about 40 Mpc) was set, in agreement with the redshift at which CCSNe are typically observed (e.g. [16]). The figure also shows $f^{\rm lim}_{\lambda,\rm USAT}$, $f^{\rm lim}_{\lambda,\rm ZTF}$, and the instrument observation bands. These results suggest that for representative RSGs and BSGs in an ambient medium with dust properties similar to those of our Galaxy, the UV emission from the SBO of either RSGs or BSGs would become visible to ULTRASAT approximately 5 minutes later. After at least 15(30) minutes, RSG(BSG) emission might also be detected by the ZTF. While the signal from RSGs remains visible in both optical and UV bands for around 6 months, the signal from BSGs is expected to last only ~3 weeks(~4 months), at which point it falls below the ULTRASAT(ZTF) detection threshold. Apparently, the much larger progenitor radius of RSG stars causes the UV and optical emission to remain widely visible for much longer as a result of the reduced cooling from expansion. The results obtained with the minimum and median extinction values are comparable. For the highest value of E_{B-V} in the 2σ range, in contrast, (i) the emission from RSGs(BSGs) becomes visible ~15(30) minutes after the SBO and (ii) BSGs remain visible to ULTRASAT for one week less.

2.2.1 Computation of event rates

Following the approach discussed in Sec. 2.2, we estimated the expected number of events per year detectable within the instrument field-of-view as a function of time after the SBO. This was computed by integrating the volumetric CCSN rate over redshift, up to the maximum redshift $z_{\rm lim}$ at which the model flux exceeds the instrument sensitivity. We adopted a standard form for the cosmic star formation rate density, and normalized to a local rate of H-rich SNe II without significant CSM, taken as 60% of the total SN II rate [17]. Full expressions and integration details can be found in [1]. We adopted the following assumptions:

- Since SNe II originate from both RSG and BSG progenitors, and the average Galactic ratio is

estimated to be BSG/RSG $\simeq 3$ [18], we assumed local rates of $R_0 = 1.1\ (2.5) \times 10^{-5}$ Mpc^{-3} yr^{-1} for RSGs (BSGs).

- To enable a direct comparison between instruments, we fixed the observation time to one hour. During this interval, ZTF can scan 3750 deg^2 of sky [19], while for ULTRASAT we adopted a strategy of four consecutive 900 s exposures, each covering its full field of view of 204 deg^2 [10]. Detection rates were further weighted by the instrument duty cycle: 100% for ULTRASAT, and 25% for ZTF, accounting for night-time operation and weather constraints [20].

As a result, Figure 2(a) shows the maximum redshift as a function of the elapsed time since the SBO from which the signal can be revealed by ULTRASAT and ZTF. The trend shows a growing horizon for a few days after the SBO, reaching a peak of $z \sim 0.24$ (~ 1.2 Gpc) for ULTRASAT and $z \sim 0.19$ (~ 920 Mpc) for ZTF if the SBO occurred roughly 4 and 10 days earlier, respectively, which later decreases. This reflects a visibility peak in the emission, as cooling light curves fade with time. At later times, only nearby SNe remain detectable. It is worth highlighting that ULTRASAT will probe larger cosmic volumes and detect events at higher redshifts. Figure 2(b) shows the corresponding number of SNe II per year detectable by ULTRASAT and the ZTF. ULTRASAT is expected to detect up to 1300 SNe II from RSGs per year, provided observations occur within ~ 4 days from the SBO, and about 65 events per year from BSGs if detected within ~ 1 day. Furthermore, ZTF may detect optical emission from about 50% of the SNe II RSG-origin seen by ULTRASAT if optical follow-up occurs within ~ 10 days after the SBO (that is, roughly one week after UV detection). In the BSG case, about one in three SNe II detected by ULTRASAT per year may also be optically observed by ZTF.

2.3 Neutrino follow-up strategies

CCSNe harbouring choked jets studied here can produce neutrinos through proton-photon interactions, which escape dense stellar envelopes and serve as early warnings for supernova explosions, enabling timely electromagnetic follow-up of SBO signals. Combining neutrino detections from telescopes like IceCube and KM3NeT with UV and optical observations offers a powerful multi-messenger approach to identify choked jets and their progenitors. ULTRASAT and ZTF can respond to neutrino alerts within a few days, extending by up to one day if neutrinos are produced deeper in the envelope [21], to optimize the chance of detecting SBO counterparts. This coordinated approach, supported by photometric and spectroscopic follow-ups, is crucial for confirming the presence of choked jets.

Based on recent constraints on the local rate of choked jets from RSGs which may substantially contribute to the observed astrophysical neutrino flux [8], and considering the IceCube upper limits [22], we estimate that up to $\sim 20\%$ detectable RSG CCSNe could host choked jets producing TeV neutrinos. With ULTRASAT expected to detect approximately 1300 RSG events per year, complemented by optical observations, multi-messenger follow-ups over several years will be essential to assess whether choked jets are a significant component of the diffuse high-energy neutrino flux.

3. Discussion and implications

Our results highlight the unique opportunity offered by coordinated UV, optical, and neutrino observations to reveal and characterize choked jets in CCSNe. In particular, we find that ULTRA-

SAT, with its wide field of view and high UV sensitivity, will be instrumental in detecting the early shock-cooling signatures that are difficult to capture with optical surveys alone. Synergy with optical instruments such as ZTF, or its successors, extends the temporal and spectral coverage, allowing for a more complete reconstruction of the emission. In parallel, real-time neutrino alerts from IceCube and KM3NeT can serve as early triggers for follow-up observations, especially valuable for events lacking a gamma-ray counterpart.

Our estimated detection rates suggest that a non-negligible fraction (~20%) of CCSNe from RSGs could harbor choked jets that produce TeV neutrinos. A multiyear monitoring campaign combining ULTRASAT, optical surveys, and neutrino observatories has the potential to either confirm or rule out choked jets as significant contributors to the diffuse high-energy neutrino background. Overall, this study supports the development of a robust multi-messenger observational strategy, and positions ULTRASAT as a key player in probing stellar explosions and the origin of high-energy cosmic neutrinos.

While this study underlines the importance of a multi-messenger strategy to improve the detectability and understanding of these events, more accurate modeling of the source physics is needed. In particular, radiative relativistic magnetohydrodynamic simulations are essential to characterize the interaction between jets and the stellar envelope in detail. Efforts are already ongoing in this direction [23]. Such simulations will complement the framework presented here by providing refined predictions for the spatial and temporal signatures of high-energy neutrinos and associated electromagnetic counterparts.

References

[1] A. Zegarelli, D. Guetta, S. Celli, S. Gagliardini, I. Di Palma, and I. Bartos, *A&A* **690** (Oct., 2024) A187.
[2] A. Zegarelli, D. Guetta, S. Celli, S. Gagliardini, I. Di Palma, and I. Bartos, *A&A* **698** (June, 2025) C1.
[3] E. Waxman and B. Katz, "Shock Breakout Theory," in *Handbook of Supernovae*, A. W. Alsabti and P. Murdin, eds., p. 967. 2017.
[4] P. Mészáros and E. Waxman, *Phys. Rev. Lett.* **87** no. 17, (Oct., 2001) 171102.
[5] **IceCube** Collaboration, M. Ackermann *et al.*, *ApJ* **799** no. 1, (Jan., 2015) 86.
[6] K. Murase, D. Guetta, and M. Ahlers, *Phys. Rev. Lett.* **116** no. 7, (Feb., 2016) 071101.
[7] H.-N. He, A. Kusenko, S. Nagataki, Y.-Z. Fan, and D.-M. Wei, *ApJ* **856** no. 2, (Apr., 2018) 119.
[8] M. Fasano, S. Celli, D. Guetta, A. Capone, A. Zegarelli, and I. Di Palma, *JCAP* **2021** no. 9, (Sept., 2021) 044.
[9] **IceCube** Collaboration, M. G. Aartsen *et al.*, *Science* **342** no. 6161, (Nov., 2013) 1242856.
[10] Y. Shvartzvald *et al.*, *ApJ* **964** no. 1, (Mar., 2024) 74.
[11] E. Waxman, P. Mészáros, and S. Campana, *ApJ* **667** no. 1, (Sept., 2007) 351–357.
[12] I. Rabinak and E. Waxman, *ApJ* **728** no. 1, (Feb., 2011) 63.
[13] N. Ganot *et al.*, *ApJ* **931** no. 1, (May, 2022) 71.
[14] L. Dessart and D. J. Hillier, *A&A* **622** (Feb., 2019) A70.
[15] J. A. Cardelli, G. C. Clayton, and J. S. Mathis, *ApJ* **345** (Oct., 1989) 245.
[16] K. Taggart and D. A. Perley, *MNRAS* **503** no. 3, (May, 2021) 3931–3952.
[17] H. Lin, J. Zhang, and X. Zhang, *Universe* **9** no. 5, (Apr., 2023) 201.
[18] P. Eggenberger, G. Meynet, and A. Maeder, *A&A* **386** (May, 2002) 576–582.
[19] E. C. Bellm *et al.*, *Publ. Astron. Soc. Pac.* **131** no. 995, (Jan., 2019) 018002.
[20] R. Dekany *et al.*, *Publ. Astron. Soc. Pac.* **132** no. 1009, (Mar., 2020) 038001.
[21] M. D. Kistler, W. C. Haxton, and H. Yüksel, *ApJ* **778** no. 1, (Nov., 2013) 81.
[22] **IceCube** Collaboration, R. Abbasi *et al.*, *ApJL* **949** no. 1, (May, 2023) L12.
[23] M. Pais, A. Zegarelli, S. Celli., and A. Peretti, E., *PoS* **ICRC2025** (2025) 1138.